U.S. DEPARTMENT OF ENERGY | Office of Science

DOE/SC-ARM/TR-148

Doppler Lidar Wind Value-Added Product

RK Newsom
C Sivaraman
TR Shippert
LD Riihimaki

July 2015

ARM
CLIMATE RESEARCH FACILITY

DISCLAIMER

DOE/SC-ARM/TR-148

Doppler Lidar Wind Value-Added Product
Version 1.0

RK Newsom
C Sivaraman
TR Shippert
LD Riihimaki

July 2015

Work supported by the U.S. Department of Energy,
Office of Science, Office of Biological and Environmental Research

Acronyms

AGL	Above-ground level
ARM	Atmospheric Radiation Measurement
CBH	Cloud-base height
DLWIND	Doppler Lidar Wind
DLWSTATS	Doppler Lidar Vertical Velocity Statistics
NAN	Not-a-number
NIR	near-infrared
PNNL	Pacific Northwest National Laboratory
PPI	plan-position-indicator
SGP	Southern Great Plains
SGPDL	Southern Great Plains Doppler lidar
SNR	signal-to-noise ratio
VAD	velocity-azimuth-display
VAP	Value-added product

Contents

Figures

Tables

1.0 Introduction

Wind speed and direction, together with pressure, temperature, and relative humidity, are the most fundamental atmospheric state parameters. Accurate measurement of these parameters is crucial for numerical weather prediction. Vertically resolved wind measurements in the atmospheric boundary layer are particularly important for modeling pollutant and aerosol transport. Raw data from a scanning coherent Doppler lidar system can be processed to generate accurate height-resolved measurements of wind speed and direction in the atmospheric boundary layer.

The Atmospheric Radiation Measurement (ARM) Climate Research Facility currently operates several scanning coherent Doppler lidar systems at various sites around globe. These instruments operate in the near-infrared (NIR, 1.5 microns) region and provide measurements of radial velocity, attenuated aerosol backscatter, and signal-to-noise ratio (SNR). The systems are operated using a fixed scan schedule consisting of plan-position-indicator (PPI) scans that are performed several times per hour. These scans are performed by scanning the beam in azimuth while maintaining a fixed elevation angle. The Doppler lidar wind (DLWIND) value-added product (VAP) reads in data from PPI scan files (i.e., *dlppi*.b1.* files) and computes vertical profiles of horizontal wind speed and direction using a method based on the traditional velocity-azimuth-display (VAD) algorithm (Browning and Wexler 1968).

2.0 Input Data

The DLWIND VAP reads in data from the <*site*>dlppi<*facility*>.b1 datastream and <site>met<facility>.b1, and parameters from one ASCII configuration file. Specific variables required from the input datastreams are listed in Table 1 and Table 2.

Table 1. Variables and Global Attributes from the <*site*>dlppi<*facility*>.b1 Datastream Used by the DLWIND VAP.

Variable Name	Description	Units
base_time	Seconds since 1970-1-1 0:00:00 0:00	sec
time_offset	Time offset from base_time	sec
range	Distance from lidar to center of range gate	m
azimuth	Beam azimuth relative to true north	deg
elevation	Beam elevation	deg
radial_velocity	Radial velocity	ms-1
intensity	Intensity (signal to noise ratio + 1)	unitless
alt	Altitude above mean sea level	m
dlat (global attribute)	Lidar latitude in double precision	deg
dlon (global attribute)	Lidar longitude in double precision	deg

Table 2. Variables and Global Attributes from the <*site*>met<*facility*>.b1 Datastream Used by the DLWIND VAP.

Variable Name	Description	Units
Atmos_pressure	Atmospheric pressure	kPa
pwd_precip_rate_mean	Present Weather Detector (PWD) 1-minute mean precipitation rate	Mm/hr
rh_mean	Relative humidity mean	%
temp_mean	Temperature mean	degC
wdir_vec_mean	Wind direction vector mean	deg
wspd_vec_mean_velocity	Wind speed vector mean	m/s
Lat	North latitude	degree_N
Lon	East longitude	degree_E
Alt	Altitude above mean sea level	m

The configuration file contains parameters used in generating quick-look plots, a threshold value for the SNR, and a table of values that gives the radial velocity precision as a function of the SNR. The precision estimates are determined through offline analysis of staring data, and are specific to a particular instrument.

3.0 Algorithm and Methodology

Estimates of the *u*, *v,* and *w* components of the wind field are computed from PPI scan data by assuming the flow to be horizontally uniform and steady at a given height above-ground level (AGL). At a fixed range from the lidar, the conical PPI scan traces out a circle centered above the lidar position, as indicated in. As the beam is scanned in azimuth, the radial velocity varies sinusoidally. The *u*, *v* and *w* components are retrieved by fitting a sinusoid to the radial velocity data; the amplitude, phase and offset of the sinusoid determine the wind speed, wind direction, and vertical velocity, respectively. The derived winds are representative of averages taken over the circumference of the circle and over the time it takes to complete a full PPI scan, which is typically between about 30 seconds and about two minutes, depending on the pulse integration time and number of beams used.

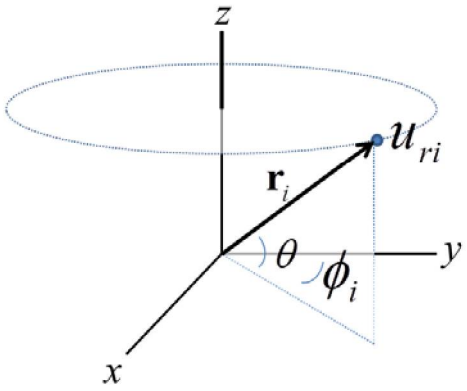

Figure 1. Geometry for Computing the Winds at a Fixed Height. The *x*, *y* and *z* axes define the east, north, and up directions, respectively. The lidar is located at the origin of the coordinate system. The position vector from the lidar to the observation point is $\mathbf{r}_i$, and u_{ri} is the radial velocity at the observation point. The elevation and azimuth angles of the observation point are θ and ϕ_i, respectively.

The fit is performed at each range gate or height by minimizing the following cost function:

$$L = \sum_i \frac{\left(\mathbf{u} \cdot \mathbf{r}_i - u_{ri}\right)^2}{\sigma_i^2}, \tag{1}$$

where $\mathbf{u}$ is the known velocity vector, u_{ri} is a radial velocity measurement, σ_i the corresponding radial velocity precision, and $\mathbf{r}_i$ is the unit vector from the lidar to the observation point, as indicated in Figure 1. The summation in equation (1) is performed over all observations at a fixed range gate.
The unknown velocity in equation (1) is given by

$$\mathbf{u} = u\hat{\mathbf{x}} + v\hat{\mathbf{y}} + w\hat{\mathbf{z}} \tag{2}$$

and the position unit vector is given by

$$\mathbf{r}_i = \cos\theta \sin\phi_i \hat{\mathbf{x}} + \cos\theta \cos\phi_i \hat{\mathbf{y}} + \sin\theta \hat{\mathbf{z}} \tag{3}$$

where $\hat{\mathbf{x}}$, $\hat{\mathbf{y}}$, and $\hat{\mathbf{z}}$ are unit vectors along the *x*, *y* and *z* axes, respectively. The velocity components *u*, *v* and *w* are assumed to be constant along the circle. Minimizing equation (1) with respect to *u*, *v* and *w* (i.e., solving $\partial L / \partial u = 0$, $\partial L / \partial v = 0$ and $\partial L / \partial w = 0$) results in a system of three equations, and three unknowns, *u*, *v* and *w*. The solution is given by

$$\begin{pmatrix} u \\ v \\ w \end{pmatrix} = \begin{pmatrix} A_{11} & A_{12} & A_{13} \\ A_{21} & A_{22} & A_{23} \\ A_{31} & A_{32} & A_{33} \end{pmatrix}^{-1} \begin{pmatrix} b_1 \\ b_2 \\ b_3 \end{pmatrix}, \tag{4}$$

where

$$A_{11} = \cos^2\theta \sum_i \sigma_i^{-2} \sin^2\phi_i \,,$$

$$A_{12} = A_{21} = \cos^2\theta \sum_i \sigma_i^{-2} \sin\phi_i \cos\phi_i \,,$$

$$A_{13} = A_{31} = \cos\theta \sin\theta \sum_i \sigma_i^{-2} \sin\phi_i \,,$$

$$A_{22} = \cos^2\theta \sum_i \sigma_i^{-2} \cos^2\phi_i \,,$$

$$A_{23} = A_{32} = \cos\theta \sin\theta \sum_i \sigma_i^{-2} \cos\phi_i \,,$$

$$A_{33} = \sin^2\theta \sum_i \sigma_i^{-2} \,,$$

and

$$b_1 = \cos\theta \sum_i u_{ri} \sigma_i^{-2} \sin\phi_i$$

$$b_2 = \cos\theta \sum_i u_{ri} \sigma_i^{-2} \cos\phi_i$$

$$b_3 = \sin\theta \sum_i u_{ri} \sigma_i^{-2} \,.$$

Uncertainty estimates for *u*, *v,* and *w* are obtained from the diagonal elements of $\mathbf{A}^{-1}$ (Press et al. 1988); i.e.,

$$\delta u^2 = \left(\mathbf{A}^{-1}\right)_{11}, \tag{5}$$

$$\delta v^2 = \left(\mathbf{A}^{-1}\right)_{22} \tag{6}$$

and

$$\delta w^2 = \left(\mathbf{A}^{-1}\right)_{33}, \tag{7}$$

where $\mathbf{A}^{-1}$ is obtained using standard numerical matrix inversion methods (i.e., interactive data language's (IDL's) invert.pro routine). The quality of the least-squares fit is assessed using the fit residual and the linear correlation coefficient. These quantities are defined as follows:

$$\text{Residual} = \sqrt{\overline{\left(\mathbf{u}\cdot\mathbf{r} - u_r\right)^2}} \tag{8}$$

$$\text{Correlation} = \frac{\overline{(\mathbf{u}\cdot\mathbf{r} - \overline{\mathbf{u}\cdot\mathbf{r}})(u_r - \overline{u_r})}}{\left(\overline{(\mathbf{u}\cdot\mathbf{r} - \overline{\mathbf{u}\cdot\mathbf{r}})^2}\right)^{1/2}\left(\overline{(u_r - \overline{u_r})^2}\right)^{1/2}} \tag{9}$$

Equations 4, 5, 6, and 7 determine the velocity components and uncertainties at a fixed height or range gate. Wind profiles (and uncertainties) are then constructed by repeating the analysis for all range gates.

An important aspect of the DLWIND VAP is uncertainty estimation. The radial velocity precision values, σ, weight the radial velocity measurements in the fitting process, and thus help reduce the effect of outliers in the end result, and enable meaningful estimation of the uncertainties in the derived velocity components.

An empirical relationship between σ and SNR is determined through an offline analysis of radial velocity and SNR time-series measurements. For a given range gate, the noise contribution to the radial velocity signal variance (i.e., the σ^2) is estimated from the auto-covariance of 30-min time series of radial velocity measurements from staring scan files as described by Lenschow et al. (2000) and Pearson et al. (2009). Noise variance estimates are then related to the mean SNR over that same 30-min period. This analysis is then repeated for all range gates and 30-minute intervals over a prescribed analysis period (typically one day). The end result is a data set consisting of σ and SNR sample pairs.

Figure 2a shows a typical scatter plot of σ^2 versus SNR, as derived from vertical staring data acquired by the SGPDL on 10 August 2013. A smoothly varying empirical curve is obtained by averaging many days of precision estimates. Figure 2b shows an example of the median precision versus SNR for the Tropical Western Pacific DL over the period from 6 March through 16 April 2015. The blue curve fit shown in Figure 2b is the data stored in the configuration file and used by the DLWIND VAP to obtain the σ values that appear in equations 1, 3,4, 5 and 6.

Figure 2 also shows that for the high SNR (roughly greater than 0.1), the radial velocity precision is well below 10 cm s^{-1}. The minimum (best) precision is approximately 4 cm s^{-1}. At very low SNR, the precision saturates due to the finite bandwidth of the receiver. In this regime, the radial velocity estimates tend to be randomly distributed between plus and minus the Nyquist velocity (19.4 ms^{-1}).

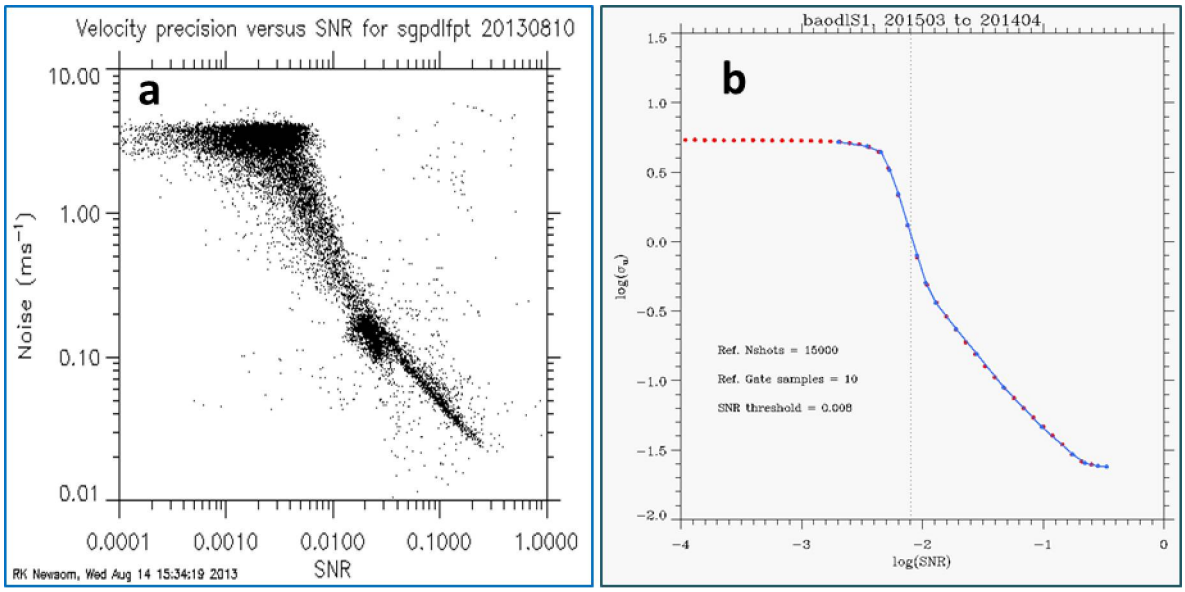

Figure 2. a) Radial Velocity Noise Standard Deviation (i.e., Precision) Estimates versus SNR for the Southern Great Plains Doppler Lidar from Time Series Analysis of Vertical Staring Data on 10 August 2013. b) The red dots represent the median radial velocity precision as a function of SNR for the Tropical Western Pacific DL for the period from 6 March through 16 April 2015. The blue curve is a curve fit.

The relationship between σ^2 and SNR depends on a number of system-specific parameters. The theoretical relationship is well described by a generalization of the Cramer-Rao lower bound due to Rye and Hardesty (1993), and is given by (Pearson 2009; O'Connor 2010)

$$\sigma^2 = \frac{1}{nM} f(SNR), \tag{10}$$

where

$$f(\alpha) = \frac{4\sqrt{\pi}\Delta v^3}{\Delta B \cdot SNR^2}\left(1 + \frac{\Delta B \cdot SNR}{2\pi\Delta v}\right)^2 \tag{11}$$

and

ΔB	=	Receiver bandwidth
Δv	=	Signal spectral width
n	=	Number of laser shots averaged
M	=	Number of digitized samples per range gate

The receiver bandwidth is given by twice the Nyquist velocity, $\Delta B = 2v_{Nyquist}$, where $v_{Nyquist} = \lambda\nu_s / 4$, λ is the wavelength, and ν_s is the A-to-D sampling rate used in the acquisition of the raw atmospheric return signal. For the ARM Doppler lidars, the wavelength is 1.548 μm, and the sampling rate is 50 MHz. Thus, the Nyquist velocity is 19.4 ms^{-1} and the receiver bandwidth is 38.8 ms^{-1}. We may regard the receiver bandwidth and the signal spectral width as fixed. However, the number of pulses averaged and the number of samples per gate can easily be changed by the operator. Since the wide-band SNR is independent of n and M (Frehlich and Yadlowsky 1994), the precision can be related to a reference value by

$$\sigma^2 = \frac{n_{ref}M_{ref}}{nM}\sigma_{ref}^2 \tag{12}$$

where σ_{ref} is the reference precision determined using n_{ref} and M_{ref}. The reference precision and corresponding SNR values are stored in the configuration. Equation (12) then provides a simple means of computing the precision appropriate to the current lidar configuration (as determined by n and M) from the reference value. We note that the ARM Doppler lidars are typically operated using a 1-sec pulse integration time (n = 15000) and a 30-m range gate (M = 10). There are, however, many cases in which other values of n and M have been used.

The configuration file for the DLVAD VAP contains a threshold value for the SNR. Radial velocity estimates corresponding to SNR values below this threshold are not used in the computation of the wind profiles. We find that a threshold value of about 0.008 works well in rejecting most of the poor-quality radial velocity data. From Figure 3 we can see that for SNR>0.008, the radial velocity precision is generally less than 1 ms^{-1}.

4.0 Output Data

The DLWIND VAP produces a single netCDF file per day. The output datastream name is <*site*>dlprofwind4news<*facility*>.c1. Fields contained in this datastream include the eastward and northward wind components (u and v, respectively), vertical velocity, and corresponding uncertainty fields. Also included are several fields that are useful for quality control, such as the mean SNR, fit residuals, and linear correlations. Metadata fields include the elapse time for the PPI scan, the elevation angle of the PPI scan, and the number of azimuth angles.

The number of profiles in a given file is equal to the number of PPI scans that were performed on that day. The height resolution of the wind profiles is dependent on the range gate size and scan elevation angle. The ARM Doppler lidars are typically operated with 30-m range gates, and PPI scans are typically performed at an elevation angle of 60°. Thus, a typical height resolution is 30sin (60°) = 26 m. In additional, the minimum range for the Doppler lidar is approximately 100 m. This results in a minimum height of about 87 m for a 60° PPI scan.

The ARM Doppler lidars operate in the NIR range and are thus sensitive to scattering from aerosol but insensitive to molecular scattering. The lidar's backscatter signal typically decreases dramatically above the atmospheric boundary layer as the aerosol concentrations fall off. As a result, good quality radial velocity measurements are primarily constrained to the lowest 2 to 3 km of the atmosphere. Thus, the DLWIND VAP is usually configured to process data up to a maximum height of 3 km.

Primary variables in the output datastream include the three wind components (u, v and w), wind speed, wind direction and corresponding uncertainty estimates. Other important variables in the output include the fit residual (equation 8), the linear correlation coefficient (equation [9]) and the mean SNR (averaged along the circumference of the circle traced out by the PPI scan at a fixed height). The primary variables will contain missing values in regions where the SNR is below threshold. Users can apply additional quality control (QC) by filtering out wind estimates corresponding to large fit residuals and/or small linear correlation coefficients. In additional, users can use the mean SNR field to apply a higher SNR threshold than was used in the original processing.

The DLWIND VAP also includes several variables from the surface meteorological instrumentation (MET) datastream. These have been included to facilitate comparison with independent measurements of wind speed and wind direction (i.e., to provide a sanity check on the lidar measurements) and to provide additional QC of the lidar measurements. The precipitation rate measurement from the surface MET station is useful for determining when the lidar measurements may be adversely affected by precipitation. A complete listing of all output variables is given in Appendix A.

4.1 Scientific Output Variables

A listing of primary variables is given in Table 3.

Table 3. DLWIND VAP primary variables.

Measurement name	Variables
easterly wind component	U
northerly wind component	v
wind speed	wind_speed
wind direction	wind_direction

4.2 Error Estimates

Section 3.0 provides a comprehensive description of how uncertainties in the wind components are determined. These uncertainty estimates are obtained by propagating the effects of random error in the radial velocity measurements, which are dominated by local oscillator shot noise. However, systematic biases (if any) are more difficult to identify and characterize, and are therefore not accounted for in the uncertainty estimates provided by the DLWIND VAP.

5.0 Summary

The DLWIND VAP uses PPI scanning data from the Doppler lidar to compute vertical profiles of wind speed and direction using a method based on the traditional velocity-azimuth-display algorithm (Browning and Wexler 1968). Primary variables in the output datastream include the three wind components (u, v and w), wind speed, wind direction, and corresponding uncertainty estimates. Uncertainty estimates are obtained by propagating the effects of random error in the radial velocity measurements.

The DLWIND VAP produces a single netCDF file per day, and one vertical profile is generated for each PPI scan performed. The ARM Doppler lidars typically perform several PPI scans per hour, and each PPI scan takes anywhere from roughly 30 seconds to two minutes to complete, depending on how the lidar is configured. As an example, a typical configuration is to perform one 8-beam PPI scan every 15 minutes. The elapse time for the 8-beam PPI is roughly 40 seconds. Thus, the output contains nominally $4 \times 24 = 96$ wind profiles, with each profile representing a 40-second average taken every 15 minutes.

The vertical resolution of the output is determined by the PPI elevation angle and the range resolution. The ARM Doppler lidars are typically operated with 30-m range gates, and PPI scans are typically performed at an elevation angle of 60°. Thus, a typical height resolution is $30\sin(60^\circ) = 26$ m. In additional, the minimum range for the Doppler lidar is approximately 100 m. This results in a minimum height of about 87 m for a 60° PPI scan.

6.0 Example Plots

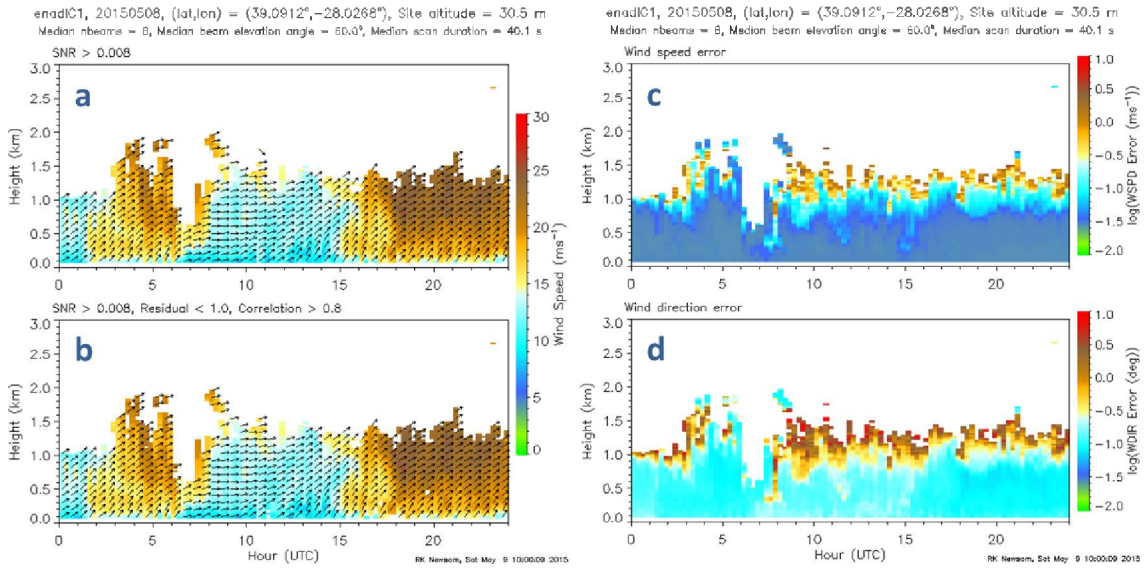

Figure 3. Sample Quicklook Plots from the Eastern North Atlantic Doppler Lidar (ENADL) on 8 May 2015. a) Wind speed (color) and wind vector direction (arrows) for SNR>0.008; b) Wind speed (color) and wind vector direction (arrows) for SNR>0.008, residual<1 ms^{-1} and correlation>0.8; c) wind speed error; d) wind direction error.

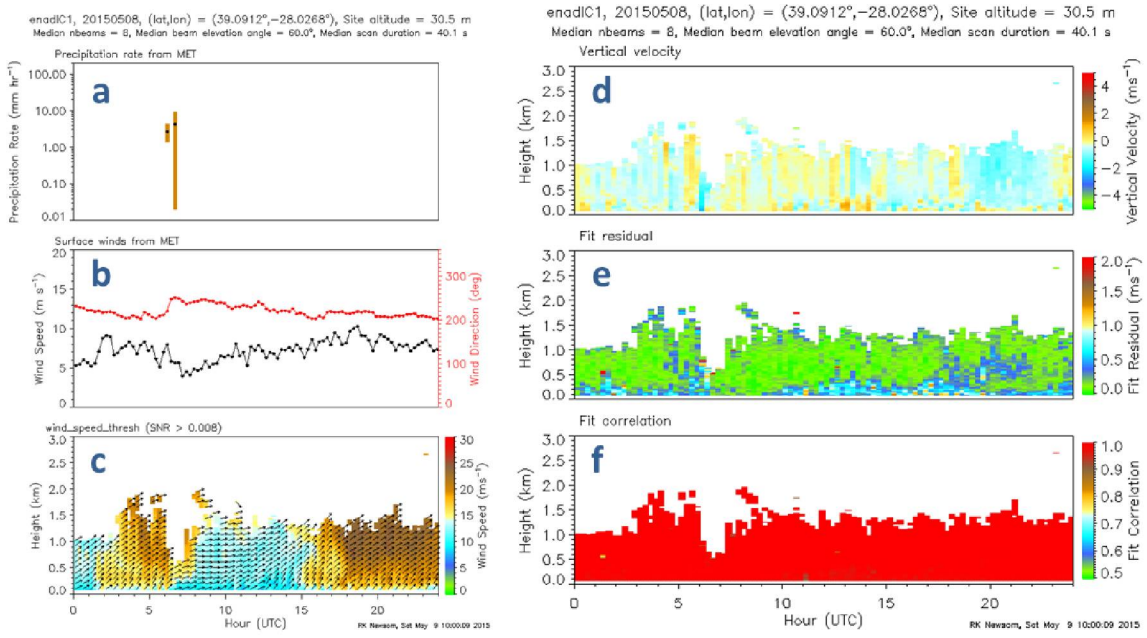

Figure 4. Sample Quicklook Plots from the ENADL on 8 May 2015. a) Precipitation rate from the surface met station; b) Wind speed (black) and wind direction (red) from the surface met station, residual<1ms^{-1} and correlation>0.8; c) Wind speed (color) and wind vector direction (arrows) for SNR>0.008; d) vertical velocity; e) fit residual; f) fit correlation.

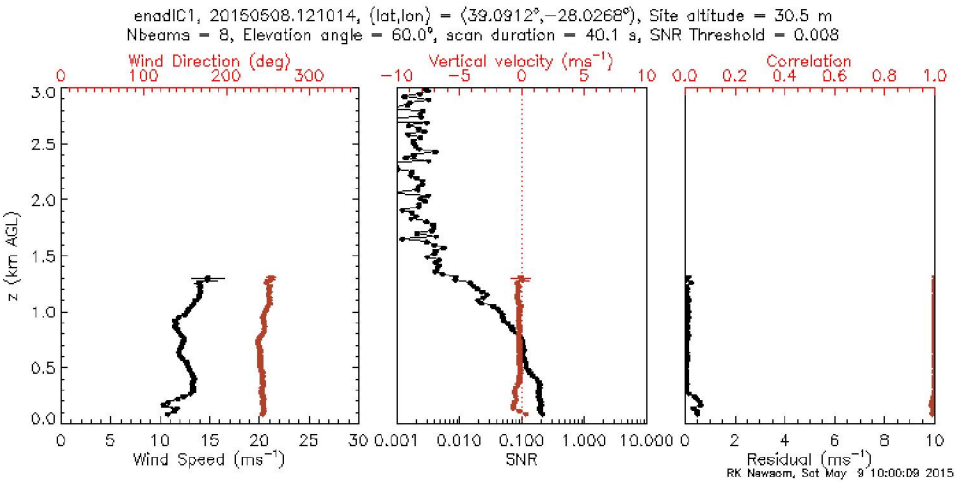

Figure 5. Sample Quicklook Plots from the ENADL at 12:10:14 UTC on 8 May 2015. The right panel shows profiles of wind speed (black) and wind direction (red). The middle panel shows profiles of the mean SNR (black) and vertical velocity (red). The right panel shows profiles of the fit residual (black) and the correlation coefficient (red).

7.0 References

Browning, K, R Wexler. 1968. The determination of kinematic properties of a wind field using Doppler radar. *Journal of Applied Meteorology*, 7, 105-113.

Frehlich, RG and MJ Yadlowsky. 1994. Performance of Mean-Frequency Estimators for Doppler Radar and LIDAR. *Journal of Atmospheric and Oceanic Technology*, 11, 1217-1230.

Lenschow, DH, V Wulfmeyer, C Senff. 2000. Measuring Second- through Fourth-Order Moments in Noisy Data. *Journal of Atmospheric and Oceanic Technology,* 17, 1330-1347.

O'Connor, EJ, AJ Illingworth, IM Brooks, CD Westbrook, RJ Hogan, F Davies, BJ Brooks. 2010. A Method for Estimating the Turbulent Kinetic Energy Dissipation Rate from a Vertically Pointing Doppler LIDAR, and Independent Evaluation from Balloon-Borne In Situ Measurements. *Journal of Atmospheric and Oceanic Technology,* 27, 1652-1664.

Pearson, G, F Davies, and C Collier. 2009. An Analysis of the Performance of the UFAM Pulsed Doppler LIDAR for Observing the Boundary Layer. *Journal of Atmospheric and Oceanic Technology*, 26, 240-250.

Press, WH, BP Flannery, SA Teukolsky, WT Vetterling. 1988. *Numerical Recipies in C*. Cambridge University Press, Cambridge, pp. 528-534.

Rye, BJ, RM Hardesty. 1993. Discrete spectral peak estimation in incoherent backscatter heterodyne Lidar. I: Spectral accumulation and the Cramer-Rao lower bound. *IEEE Transactions on Geoscience and Remote Sensing*, 31, 16–27.

Appendix A

Output Data

Appendix A

Output Data

```
netcdf sgpdlprofwind4newsC1.c1.20150421.000644 {
dimensions:
        time = UNLIMITED ; // (94 currently)
        height = 164 ;
        bound = 2 ;
variables:
        int base_time ;
                base_time:string = "2015-04-21 00:00:00 0:00" ;
                base_time:long_name = "Base time in Epoch" ;
                base_time:units = "seconds since 1970-1-1 0:00:00 0:00" ;
                base_time:ancillary_variables = "time_offset" ;
        double time_offset(time) ;
                time_offset:long_name = "Time offset from base_time" ;
                time_offset:units = "seconds since 2015-04-21 00:00:00 0:00" ;
                time_offset:ancillary_variables = "base_time" ;
        double time(time) ;
                time:long_name = "Time offset from midnight" ;
                time:units = "seconds since 2015-04-21 00:00:00 0:00" ;
                time:bounds = "time_bounds" ;
        double time_bounds(time, bound) ;
        float height(height) ;
                height:long_name = "Height above ground level" ;
                height:units = "m" ;
                height:standard_name = "height" ;
        float scan_duration(time) ;
                scan_duration:long_name = "PPI scan duration" ;
                scan_duration:units = "second" ;
                scan_duration:missing_value = -9999.f ;
        float elevation_angle(time) ;
                elevation_angle:long_name = "Beam elevation angle" ;
                elevation_angle:units = "degree" ;
                elevation_angle:missing_value = -9999.f ;
        short nbeams(time) ;
                nbeams:long_name = "Number of beams (azimuth angles) used in wind vector
estimation" ;
                nbeams:units = "unitless" ;
        float u(time, height) ;
                u:long_name = "Eastward component of wind vector" ;
                u:units = "m/s" ;
                u:missing_value = -9999.f ;
        float u_error(time, height) ;
                u_error:long_name = "Estimated error in eastward component of wind vector" ;
                u_error:units = "m/s" ;
                u_error:missing_value = -9999.f ;
        float v(time, height) ;
```

```
        v:long_name = "Northward component of wind vector" ;
        v:units = "m/s" ;
        v:missing_value = -9999.f ;
    float v_error(time, height) ;
        v_error:long_name = "Estimated error in northward component of wind vector" ;
        v_error:units = "m/s" ;
        v_error:missing_value = -9999.f ;
    float w(time, height) ;
        w:long_name = "Vertical component of wind vector" ;
        w:units = "m/s" ;
        w:missing_value = -9999.f ;
    float w_error(time, height) ;
        w_error:long_name = "Estimated error in vertical component of wind vector" ;
        w_error:units = "m/s" ;
        w_error:missing_value = -9999.f ;
    float wind_speed(time, height) ;
        wind_speed:long_name = "Wind speed" ;
        wind_speed:units = "m/s" ;
        wind_speed:missing_value = -9999.f ;
    float wind_speed_error(time, height) ;
        wind_speed_error:long_name = "Wind speed error" ;
        wind_speed_error:units = "m/s" ;
        wind_speed_error:missing_value = -9999.f ;
    float wind_direction(time, height) ;
        wind_direction:long_name = "Wind direction" ;
        wind_direction:units = "degree" ;
        wind_direction:missing_value = -9999.f ;
    float wind_direction_error(time, height) ;
        wind_direction_error:long_name = "Wind direction error" ;
        wind_direction_error:units = "degree" ;
        wind_direction_error:missing_value = -9999.f ;
    float residual(time, height) ;
        residual:long_name = "Fit residual" ;
        residual:units = "m/s" ;
        residual:missing_value = -9999.f ;
    float correlation(time, height) ;
        correlation:long_name = "Fit correlation coefficient" ;
        correlation:units = "unitless" ;
        correlation:missing_value = -9999.f ;
    float mean_snr(time, height) ;
        mean_snr:long_name = "Signal to noise ratio averaged over nbeams" ;
        mean_snr:units = "unitless" ;
        mean_snr:missing_value = -9999.f ;
    float snr_threshold ;
        snr_threshold:long_name = "SNR threshold" ;
        snr_threshold:units = "unitless" ;
        snr_threshold:missing_value = -9999.f ;
    float met_wspd(time) ;
        met_wspd:long_name = "Vector mean surface wind speed from MET" ;
        met_wspd:units = "m/s" ;
        met_wspd:missing_value = -9999.f ;
```

```
            met_wspd:cell_methods = "time: mean" ;
        float met_wdir(time) ;
            met_wdir:long_name = "Vector mean surface wind direction from MET" ;
            met_wdir:units = "degree" ;
            met_wdir:missing_value = -9999.f ;
            met_wdir:cell_methods = "time: mean" ;
        float met_spr(time) ;
            met_spr:long_name = "Mean surface precipitation rate during averaging period from
MET" ;
            met_spr:units = "mm/hr" ;
            met_spr:missing_value = -9999.f ;
            met_spr:cell_methods = "time: mean" ;
        float met_spr_min(time) ;
            met_spr_min:long_name = "Minimum surface precipitation rate during averaging
period from MET" ;
            met_spr_min:units = "mm/hr" ;
            met_spr_min:missing_value = -9999.f ;
            met_spr_min:cell_methods = "time: minimum" ;
        float met_spr_max(time) ;
            met_spr_max:long_name = "Maximum surface precipitation rate during averaging
period from MET" ;
            met_spr_max:units = "mm/hr" ;
            met_spr_max:missing_value = -9999.f ;
            met_spr_max:cell_methods = "time: maximum" ;
        float met_dt ;
            met_dt:long_name = "Averaging period length used for MET data" ;
            met_dt:units = "second" ;
            met_dt:missing_value = -9999.f ;
        float met_lat ;
            met_lat:long_name = "MET latitude" ;
            met_lat:units = "degree_N" ;
            met_lat:missing_value = -9999.f ;
            met_lat:standard_name = "latitude" ;
        float met_lon ;
            met_lon:long_name = "MET longitude" ;
            met_lon:units = "degree_E" ;
            met_lon:missing_value = -9999.f ;
            met_lon:standard_name = "longitude" ;
        float met_alt ;
            met_alt:long_name = "MET altitude" ;
            met_alt:units = "m" ;
            met_alt:missing_value = -9999.f ;
            met_alt:standard_name = "altitude" ;
        float lat ;
            lat:long_name = "North latitude" ;
            lat:units = "degree_N" ;
            lat:valid_min = -90.f ;
            lat:valid_max = 90.f ;
            lat:standard_name = "latitude" ;
        float lon ;
            lon:long_name = "East longitude" ;
```

```
            lon:units = "degree_E" ;
            lon:valid_min = -180.f ;
            lon:valid_max = 180.f ;
            lon:standard_name = "longitude" ;
        float alt ;
            alt:long_name = "Altitude above mean sea level" ;
            alt:units = "m" ;
            alt:standard_name = "altitude" ;

// global attributes:
            :process_version = "vap-dlprof_wind-0.4-0.el6" ;
            :command_line = "idl -D 0 -R -n dlprof_wind -s sgp -f C1 -d 20150421" ;
            :dod_version = "dlprofwind4news-c1-1.0" ;
            :Conventions = "ARM-1.1" ;
            :site_id = "sgp" ;
            :platform_id = "dlprofwind4news" ;
            :location_description = "Southern Great Plains (SGP), Lamont, Oklahoma" ;
            :datastream = "sgpdlprofwind4newsC1.c1" ;
            :data_level = "c1" ;
            :facility_id = "C1" ;
            :input_datastreams = "sgpdlppiC1.b1 : 2.10 : 20150421.000624-
20150421.234538\n",
                    "sgpmetE13.b1 : 4.28 : 20150420.000000-20150422.000000" ;
            :dlat = "36.60530" ;
            :dlon = "-97.48649" ;
            :serial_number = "0710-07" ;
            :doi = "DOI:10.5439/1178582" ;
            :doi_url = "http://dx.doi.org/10.5439/1178582" ;
            :history = "created by user dsmgr on machine ruby at 2015-05-21 20:42:26, using
vap-dlprof_wind-0.4-0.el6" ;
```

www.arm.gov

U.S. DEPARTMENT OF
ENERGY

Office of Science